The 9th European Congress on Computational Methods in Applied Sciences and Engineering
ECCOMAS Congress 2024
3–7 June 2024, Lisboa, Portugal

MATHEMATICAL MODELING OF DAMAGE-PLASTICITY CONCRETE MATERIAL MODEL SUBJECTED TO HIGH-STRAIN RATE LOADING ECCOMAS CONGRESS 2024

Sobhan Pattajoshi[1], **Sonalisa Ray**[2]

[1] Civil Engineering Department, Indian Institute of Technology, Roorkee, India,
sobhan_p@ce.iitr.ac.in

[2] Civil Engineering Department, Indian Institute of Technology, Roorkee, India,
sonalisa.ray@ce.iitr.ac.in

Key words: RCC Slab, Projectile Impact, User Subroutine, Material Modeling, Damage Model, Failure Mode

Summary. The Riedel, Hiermaier, and Thoma (RHT) model, a concrete material model, is primarily utilized for impact and explosive analysis involving high strain rates. While the original RHT model yielded sufficiently comparable results for penetration depth, it exhibited limitations in accurately representing the dynamic response of concrete, particularly in underestimating tension damage (spalling). Previous studies aimed at enhancing the RHT model have focused on adjusting the input parameters to better approximate experimental data. In this study, we propose a model designed to address the shortcomings related to dynamic tensile failure behaviour in the original RHT model. Our approach involves incorporating user-defined functions, allowing for improved representation of the concrete dynamic response, especially in the context of tensile failure. The model accuracy was validated through single-element simulations. The viability of the numerical simulation algorithm has also been verified for projectile penetration. After validation, the study examines how projectile penetration influences the damage. Numerical results illustrate that damage resulting from projectile penetration significantly influences the failure mode and stress wave propagation of the target. The results confirmed that the developed constitutive model could well describe the dynamic behaviour of the RCC slab under projectile impact. The research findings offer crucial insights for designing protective structures against projectile penetration.

1 INTRODUCTION

Concrete is a composite material comprising various aggregates and admixtures tailored to specific purposes, rendering it heterogeneous in its properties. It has been a primary material in the construction and defence industries for decades due to its impressive compressive strength, durability, fire resistance, and water resistance. These attributes enable the construction of stable structures with excellent performance characteristics. Recent research endeavours have focused on enhancing the strength of concrete by integrating various reinforcement materials [1]. However, it's crucial to note an essential aspect of concrete mechanical behaviour: its susceptibility to cracking under tensile stress. The inherent brittleness of concrete means that once

cracks develop, the protective capabilities of the structure diminish significantly, compromising safety. In scenarios involving high-velocity impact loads such as blast pressure or collisions, the fracture mechanism of concrete primarily involves tensile failure due to crack propagation. This can lead to phenomena like spalling or scabbing, resulting in the generation of fragments or debris from the structure, posing risks of personal or physical harm. Understanding the behaviour of concrete under high strain rates and tensile loads is paramount due to its implications for structural integrity and safety. Therefore, comprehensive research efforts are essential in this regard.

Conducting experiments under dynamic loads presents challenges in establishing suitable experimental environments and limitations in capturing instantaneous phenomena. Hence, an alternative approach involves predicting experimental outcomes or structural behaviour using hydrocode numerical analysis [2, 3, 4, 5, 6, 7, 8, 9]. An advanced constitutive model is vital to accurately depict the dynamic tensile behaviour of concrete, including crack formation and dynamic fracture. Such a model should describe the material elastoplastic state using a yield surface and be capable of expressing nonlinear hardening and softening behaviour upon the stress state [10]. Moreover, it should reflect the reduced tensile load-bearing capacity from crack formation. Over the past decades, numerous yield criteria have been proposed to illustrate the behaviour of brittle materials under diverse loading conditions [11, 12, 13, 14, 15]. However, these models cannot often depict time-dependent dynamic behaviour under high-impact loads [16, 17, 18, 19]and the associated softening phenomenon attributable to crack-induced stiffness reduction [20, 21, 22]. Recent advancements in modeling have endeavoured to address these limitations by defining yield surfaces based on variables capable of elucidating such phenomena [23, 24, 25]. Notably, the RHT model [25] stands out as the most prevalent material model for concrete, integrated into commercial software and primarily utilized for impact and penetration analyses involving high strain rates.

In this study, a crack softening model has been integrated into the default RHT material model to enhance the representation of dynamic tensile behaviour in concrete. Initially, single-element simulations were conducted to validate the accuracy of the modified damage model. Subsequently, numerical simulations were carried out using this modified damage model. The integration of the crack softening model into the RHT material model represents a significant advancement in accurately modeling and predicting the dynamic response of concrete structures, thereby contributing to improved safety and performance in engineering applications.

2 RIEDEL–HIERMAIER–THOMA (RHT) MATERIAL MODEL

The Riedel–Hiermaier–Thoma (RHT) model is commonly employed to analyse concrete behaviour [26]. This model incorporates pressure hardening, strain hardening, strain rate hardening, strain softening, and third invariant dependence of concrete. It delineates three pressure-dependent surfaces within stress space, namely the elastic limit surface, failure surface, and residual surface. In the elastic region, the elastic limit surface equation ($Y_{elastic}$) governs the behaviour under elastic stresses. The boundary conditions for this surface are set using the parabolic cap function (F_{cap}), which incorporates the porous equation of state ($p - \alpha$) at higher pressures to account for pore compaction. As stresses increase, strain hardening occurs until the material reaches the failure surface ($Y_{failure}$). Beyond the failure surface, the post-failure surface ($Y_{fracture}$) is determined by interpolating between the failure surface and residual surface

using a damage index (D). The elastic limit surface ($Y_{elastic}$) is derived by scaling down from the failure surface ($Y_{failure}$).

$$Y_{elastic} = Y_{failure} \times F_{elastic} \times F_{cap} \tag{1}$$

$$F_{elastic} = \frac{\sigma_{t,elastic}}{\sigma_{t,ultimate}} \; or \; \frac{\sigma_{c,elastic}}{\sigma_{c,ultimate}} \tag{2}$$

Where, $\sigma_{t,elastic}$ is the elastic strength along the radial path in tension and $\sigma_{t,ultimate}$ is the failure strength along the radial path in tension. The failure surface equation is expressed below:

$$Y_{failure} = Y_{TXC}(p*) \times R_3(\theta) \times F_{rate}(\dot{\varepsilon}) \tag{3}$$

Where, Y_{TXC} , P^*, R_3, q, and $F_{rate}(\dot{\varepsilon})$ is the compressive meridian, normalized pressure (P/f_c), third invariant dependence term, lode angle and dynamic increase factor respectively.

$$\begin{aligned} F_{rate}(\dot{\varepsilon}) = DIF \; &= \left[\frac{\dot{\varepsilon}}{\dot{\varepsilon}_0}\right]^{\alpha} \; for \; compression \; (P^* > \tfrac{1}{3}) \\ &= \left[\frac{\dot{\varepsilon}}{\dot{\varepsilon}_0}\right]^{\delta} \; for \; tension \; (P^* < \tfrac{1}{3}) \end{aligned} \tag{4}$$

Where DIF, α and δ are the dynamic increase factor, compressive strain rate exponent and tensile strain rate exponent, respectively. The residual surface equation is presented below.

$$Y_{Residual} = B \times (P^*)^m \tag{5}$$

The parameters B and m in the RHT model are constants determined through curve fitting of experimental data [5] and do not possess dimensions. They play a crucial role in determining the residual strength of the concrete material. The fracture strength constant (B) signifies the intrinsic strength of the material and its ability to endure high-stress levels before fracturing. It reflects the material's resistance to deformation and fracture, being specific to each material. Different materials exhibit distinct fracture strength constants due to their unique mechanical properties. B helps establish the critical stress level at which the material will undergo fracture, particularly under dynamic loading conditions, thus aiding in understanding material behaviour during impact events. On the other hand, the fracture strength exponent (m) indicates the material's sensitivity to the loading rate or strain rate concerning its fracture strength. It describes how the material's strength varies under different loading rates, enabling the RHT model to adapt to diverse loading conditions. As materials may display differing fracture behaviours under dynamic loading, the exponent accommodates these variations. The post-failure surface equation is derived by linearly interpolating between the failure surface ($Y_{failure}$) and the residual surface ($Y_{residual}$), incorporating a damage factor (D) in the process. This interpolation accounts for the progressive deterioration of material strength beyond the failure point, reflecting the material's evolving behaviour as damage accumulates.

$$Y_{fractured} = (1 - D)\; Y_{failure} + D\; Y_{residual} \tag{6}$$

D is the damage parameter and is expressed as follows:

$$\begin{aligned} D \; &= \sum \frac{\Delta\varepsilon_p}{\Delta\varepsilon_p^{failure}} \quad for \; \varepsilon_p^{failure} > \varepsilon_{fmin} \\ &= \sum \frac{\Delta\varepsilon_p}{\Delta\varepsilon_{fmin}} \quad for \; \varepsilon_p^{failure} \leq \varepsilon_{fmin} \end{aligned} \tag{7}$$

$$\Delta\varepsilon_P^{failure} = D_1(P^* - P^*_{spall})^{D_2} \tag{8}$$

P^*_{spall} is the hydrodynamic tensile stress limit (f_t/f_c) which must be normalized by the uniaxial compressive strength of the material. $\Delta\varepsilon_p$ is the plastic strain increment. P^* normalized pressure. D_1 and D_2 are the shape parameters and ε_{fmin} is the failure strain.

3 DAMAGE MODEL MODIFICATION

In this section, crack softening failure is adopted. It is a fracture energy-based damage model that gradually reduces the capacity of elements to bear tensile stress as cracks develop. This model typically employs a smeared-crack approach, where the crack extends over a distance equal to the characteristic length of the element and activates once the tensile strength threshold is reached. Key parameters, such as fracture energy and tensile strength, must be determined to define the softening linear slope and are represented in the stress-strain curve by the cohesive traction-separation law. The tensile strength is a variable influencing crack formation, triggered when the maximum principal tensile stress surpasses the concrete tensile strength. Meanwhile, fracture energy determines the critical fracture strain the material can endure without failure. These parameters are crucial in defining the dynamic fracture behaviour of concrete in the crack softening model.

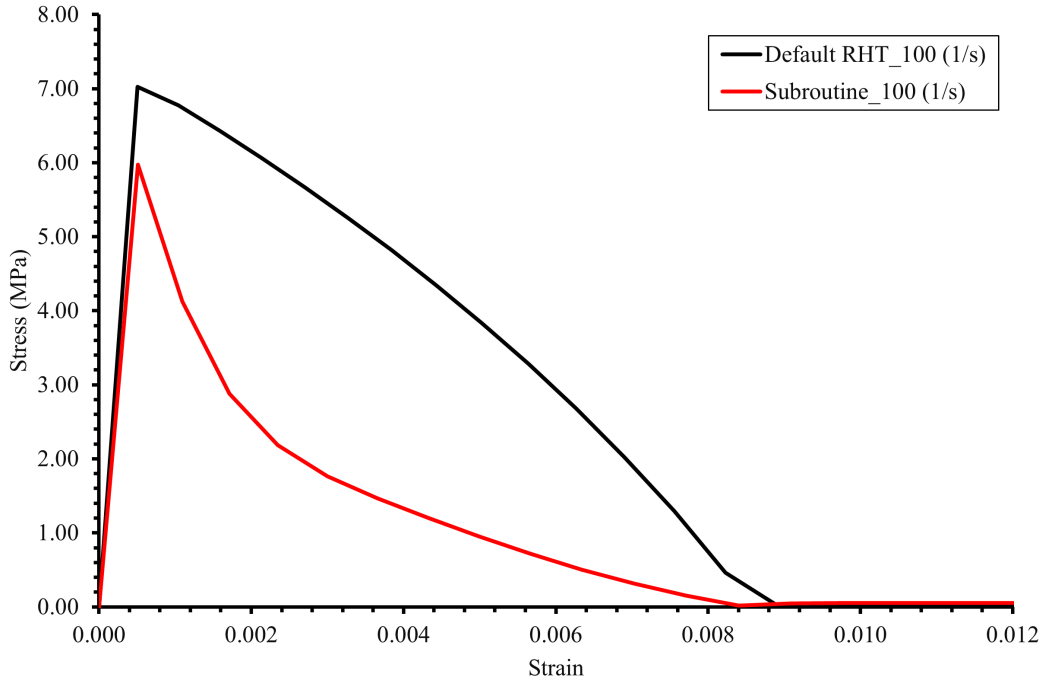

Figure 1: Single element tensile stress-strain plot comparison of default RHT model with the modified model.

Upon reaching tensile strength, it is essential to use nonlinear forms, as observed in experiments, rather than a linear stress-strain curve for softening behaviour. Experimental results, such as those from split-Hopkinson pressure bars tests, show that the stress-strain curve for concrete tensile softening resembles an exponential function. The exponential form is advantageous because it reflects a larger fracture strain for the same fracture energy compared to the linear form. Thus, it is necessary to develop an improved concrete tensile fracture model. A

modified tensile crack softening model is proposed for better modeling of brittle materials in the tensile region. Based on experimental results, the power function [27] is adopted (specifically, the Hordijk-Reinhard expression) as follows:

$$D_{\text{crack}} = 1 - \left(1 + \left(c_1 \frac{\lambda}{\varepsilon_{\text{frac}}}\right)^3\right) \exp\left(-c_2 \frac{\lambda}{\varepsilon_{\text{frac}}}\right) + \frac{\lambda}{\varepsilon_{\text{frac}}} \left(1 + c_1^3\right) \exp\left(-c_2\right) \tag{9}$$

Where $\varepsilon_{\text{frac}}$ represents the fracture strain, λ is the plastic strain increment, and $c_1 = 3.0$ and $c_2 = 6.93$ are constants derived from tensile test data for concrete. After implementing the modified damage model via a user-subroutine, the resulting tensile stress-strain curve for a single element was obtained for a strain rate of 100 s^{-1}. This curve was then compared with the default RHT model, as illustrated in Fig. 1. It is evident that the post-peak behaviour, following the application of the modified damage model, now adheres to an exponential function as defined by Eq. 9.

4 RESULTS AND DISCUSSION

In the initial analysis phase, Hanchak et al. [28] experimented to validate a mono-layer numerical model. They utilized an ogival-nose steel projectile with a caliber of 30 mm and an ogive radius of 76.2 mm, impacting targets at velocities ranging from 330 m/s to 1100 m/s. The projectile weighed 0.50 kg. The targets were reinforced concrete with strengths of 48 MPa and 140 MPa. These concrete targets measured 610 mm × 610 mm × 178 mm and were reinforced with 5.69 mm diameter steel bars spaced at 76.2 mm c/c in both in-plane and out-of-plane directions. The projectile is modelled as rigid material because little erosion was observed after the perforation test. The element size of the concrete slab is set as 2 mm × 2 mm for the FE method. After conducting the mesh convergence study for the concrete slab, a mesh size of 2mm was determined to be optimal. This finding suggests that further refining the mesh beyond this point does not significantly alter the results obtained from the simulations. This approach aimed to capture the complex interactions between the projectile and the reinforced concrete target, providing valuable insights into the dynamic behaviour of the material under impact conditions.

Pattajoshi (2024) performed a comprehensive comparative analysis between the impact damage areas obtained experimentally [28] and those predicted through numerical simulations [5], as illustrated in Fig. 2. The dimensions of craters predicted numerically closely match the experimental findings. Notably, there is a noticeable decrease in the area of spalling damage in the numerical predictions compared to the experimental results. A clear correlation emerged after examining the experimentally observed difference in spalling damage for concrete strengths of 48 MPa and 140 MPa. This correlation aligns with the well-established principle that the tensile strength of concrete decreases as its compressive strength increases [29]. Interestingly, a distinct pattern emerged from the results obtained through numerical simulations. Specifically, spalling damage was significantly more pronounced in craters formed from concrete with a strength of 48 MPa than those of 140 MPa. This inconsistency can be attributed to the parameter governing concrete spalling damage in the RHT material model.

To accurately replicate spalling damage, it is crucial to modify the damage model as discussed in the previous section. Numerical results of projectile impact tests were performed to replicate experimental investigations on concrete targets with strengths of 48 MPa and 140 MPa.

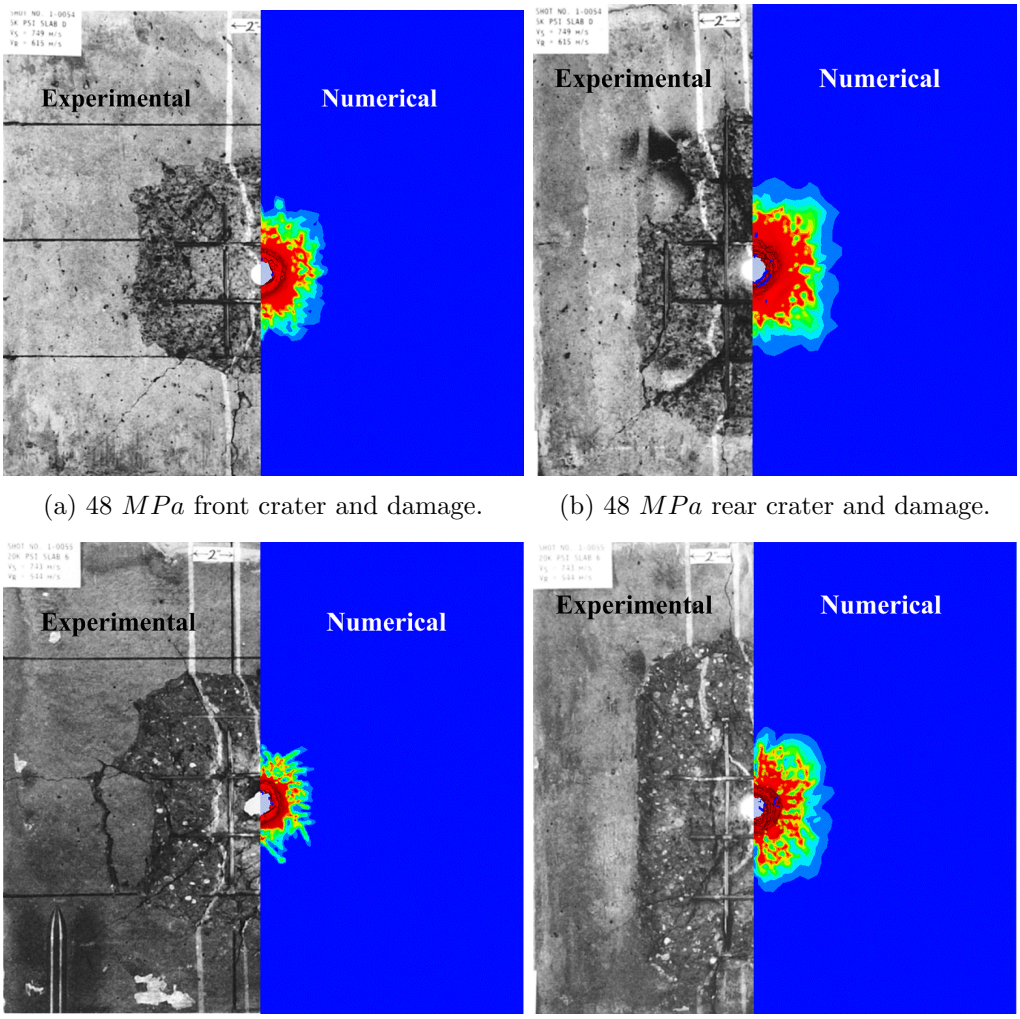

(a) 48 MPa front crater and damage. (b) 48 MPa rear crater and damage.

(c) 140 MPa front crater and damage. (d) 140 MPa rear crater and damage.

Figure 2: Experimental (Hanchak et al.) and numerical simulation comparison of front and rear damage area.

These tests were conducted using both the default RHT model and the modified damage model. The modified damage model demonstrates significant improvements in accurately capturing the spalling damage. In both cases, for concrete strengths of 48 MPa and 140 MPa, the damage diameter is notably enhanced, as presented in Fig. 3. This modification addresses the earlier drawback where damage was not as pronounced in the higher strength concrete. According to the well-established principle that the tensile strength of concrete decreases as its compressive strength increases, it is expected that the spalling damage should be more evident in the 140 MPa concrete compared to the 48 MPa concrete. The red portion in the damage contour is now more pronounced in the simulations with the modified damage model. This improvement highlights the enhanced capability of the modified model in capturing the tensile spalling damage, thereby overcoming the limitations of the default RHT model.

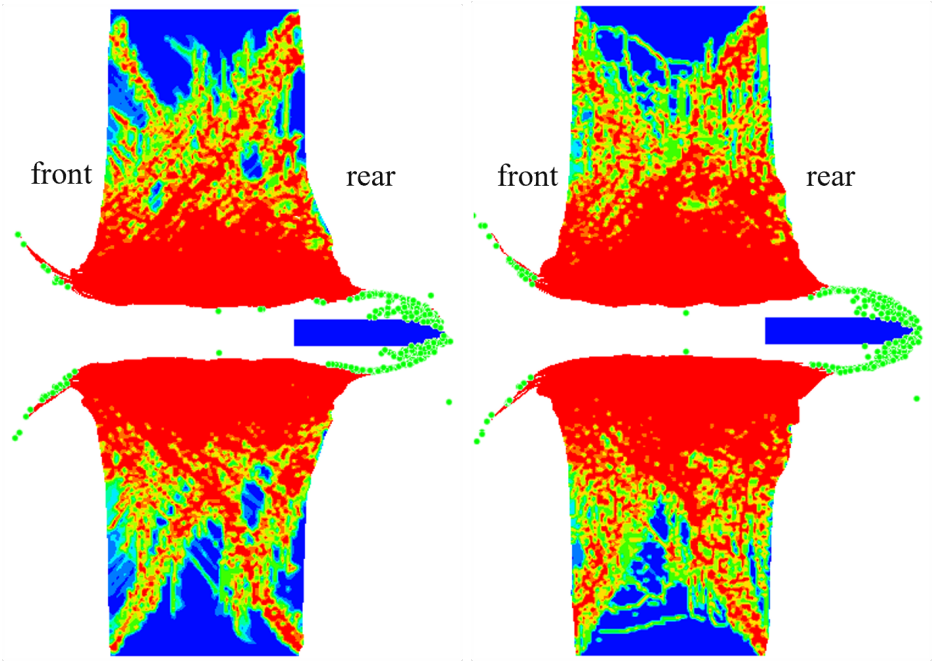

(a) 48 MPa (default RHT model). (b) 48 MPa (modified damage model).

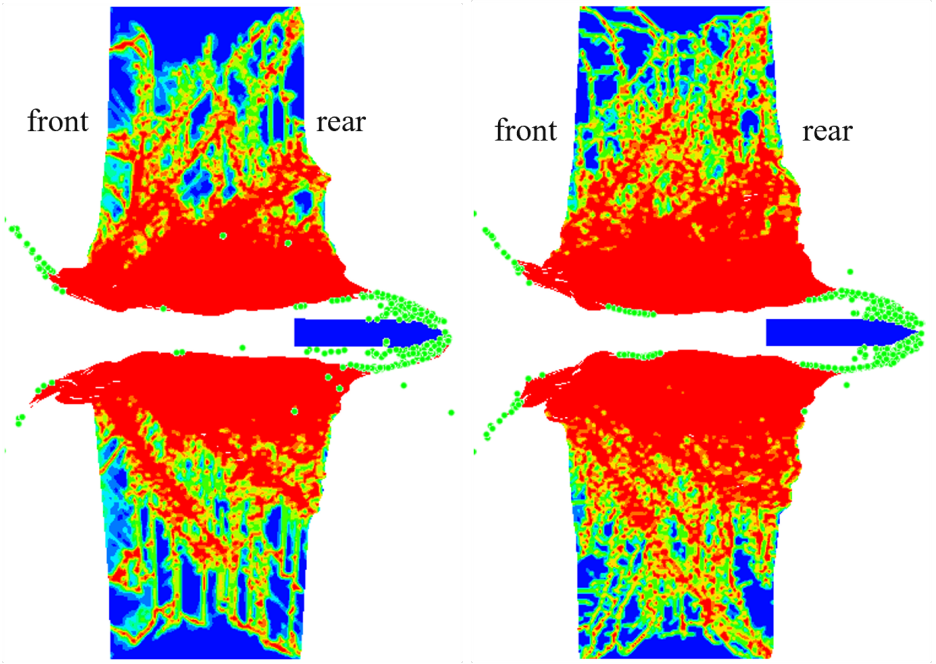

(c) 140 MPa (default RHT model). (d) 140 MPa (modified damage model).

Figure 3: Comparison of the damage area.

For a concrete strength of 48 MPa at an impact velocity of 749 m/s, the residual velocities observed are as follows: Hanchak et al. reported 615 m/s, the default RHT model yielded 625.25

m/s (an increase of 1.67%), and the modified damage model showed 625.38 m/s (an increase of 1.69%). In contrast, for a concrete strength of 140 MPa at an impact velocity of 743 m/s, the residual velocities are 544 m/s according to Hanchak et al., 607.47 m/s (an increase of 11.67%) for the default RHT model, and 605.35 m/s (an increase of 11.28%) for the modified damage model.

5 CONCLUSIONS

The RHT concrete model is widely recognized in impact and explosive simulations for its ability to capture essential properties of brittle materials under high dynamic loads. Despite its widespread use, researchers have identified limitations in accurately representing concrete strain rate-dependent dynamic behaviour. They have noted that it tends to overestimate the load capacity of elements due to its assumption of perfectly plastic behaviour under triaxial tensile loads. To address these shortcomings, previous studies have attempted to adjust the input parameters of the RHT model to better align with experimental data or numerical analysis results. However, these ad-hoc approaches have only provided solutions tailored to specific problems, highlighting the need for a more systematic methodology to enhance the RHT material model. Therefore, it is necessary to develop a comprehensive methodology to address the limitations of the original RHT model and improve its accuracy in simulating the dynamic fracture behaviour of concrete under high-speed loading conditions. Such an approach would enable more reliable and generalizable results in impact and explosive simulations. Therefore, this paper introduces a modified tensile spalling damage model aimed at enhancing the material model through the use of the Autodyn user-subroutine, which allows for user-defined functions. This enhancement leads to more accurate predictions of damage diameter and contour, resulting in a more realistic representation of concrete behavior. It is anticipated that this study will significantly contribute to the field of material modeling and provide more reliable results for future research.

REFERENCES

[1] J.-H. Song, H.-C. Eun, Improvement of flexural and shear strength of rc beam reinforced by glass fiber-reinforced polyurea (gfrpu), Civil Engineering Journal 7 (3) (2021) 407–418.

[2] C. E. Anderson Jr, An overview of the theory of hydrocodes, International journal of impact engineering 5 (1-4) (1987) 33–59.

[3] W. Sun, Z. Shi, B. Chen, J. Feng, Numerical study on rc multilayer perforation with application to ga-bp neural network investigation, Civ. Eng. J 6 (2020) 806–819.

[4] ANSYS Inc., ANSYS Autodyn User Manual 2022 R2, ANSYS Inc., Canonsburg, PA, USA (2022).

[5] S. Pattajoshi, S. Ray, Y. K. Joshi, Dynamic behaviour of multi-layer composite against single and multiple projectile impact loading, Theoretical and Applied Fracture Mechanics 129 (2024) 104189.

[6] S. Pattajoshi, S. Ray, Dynamic fracture behavior of layered composite under high strain rate loading, in: International Symposium on Plasticity and Impact Mechanics, Springer, 2022, pp. 305–322.

[7] J. C. Kishen, A. Ramaswamy, S. Ray, et al., Computational modeling of dynamic fracture of layered composite under various strain-rate loading.

[8] S. Kapoor, S. Ray, J. P. Sahoo, Y. K. Joshi, Optimization of multi-layered composites against ballistic impact: A mesoscale approach, Composite Structures 338 (2024) 118097.

[9] S. Kapoor, S. Ray, Optimization of multi-layered composite structures against impact loading, in: International Symposium on Plasticity and Impact Mechanics, Springer, 2022, pp. 269–284.

[10] R. D. Krieg, D. Krieg, Accuracies of numerical solution methods for the elastic-perfectly plastic model (1977).

[11] B. Bresler, K. S. Pister, Strength of concrete under combined stresses, in: Journal Proceedings, Vol. 55, 1958, pp. 321–345.

[12] D. C. Drucker, W. Prager, Soil mechanics and plastic analysis or limit design, Quarterly of applied mathematics 10 (2) (1952) 157–165.

[13] K. William, Warnke. constitutive model for the triaxial behavior of concrete, Proceedings, international association for bridge and structural 19 (1975).

[14] N. S. Ottosen, A failure criterion for concrete, Journal of the Engineering Mechanics Division 103 (4) (1977) 527–535.

[15] S. Hsieh, E. Ting, W. Chen, A plastic-fracture model for concrete, International Journal of Solids and Structures 18 (3) (1982) 181–197.

[16] Q. Li, H. Meng, About the dynamic strength enhancement of concrete-like materials in a split hopkinson pressure bar test, International Journal of solids and structures 40 (2) (2003) 343–360.

[17] I. Shkolnik, Influence of high strain rates on stress–strain relationship, strength and elastic modulus of concrete, Cement and Concrete Composites 30 (10) (2008) 1000–1012.

[18] X. Chen, S. Wu, J. Zhou, Quantification of dynamic tensile behavior of cement-based materials, Construction and Building Materials 51 (2014) 15–23.

[19] G. Ren, H. Wu, Q. Fang, J. Liu, Effects of steel fiber content and type on dynamic compressive mechanical properties of uhpcc, Construction and building materials 164 (2018) 29–43.

[20] A. Hillerborg, The theoretical basis of a method to determine the fracture energy gf of concrete, Materials and structures 18 (1985) 291–296.

[21] N. Bićanić, C. Pearce, Computational aspects of a softening plasticity model for plain concrete, Mechanics of Cohesive-frictional Materials: An International Journal on Experiments, Modelling and Computation of Materials and Structures 1 (1) (1996) 75–94.

[22] X. Chen, J. Bu, L. Xu, Effect of strain rate on post-peak cyclic behavior of concrete in direct tension, Construction and Building Materials 124 (2016) 746–754.

[23] T. J. Holmquist, G. R. Johnson, A computational constitutive model for glass subjected to large strains, high strain rates and high pressures (2011).

[24] L. J. Malvar, J. E. Crawford, J. W. Wesevich, D. Simons, A plasticity concrete material model for dyna3d, International journal of impact engineering 19 (9-10) (1997) 847–873.

[25] W. Riedel, K. Thoma, S. Hiermaier, E. Schmolinske, Penetration of reinforced concrete by beta-b-500 numerical analysis using a new macroscopic concrete model for hydrocodes, in: Proceedings of the 9th International Symposium on the Effects of Munitions with Structures, Vol. 315, Berlin-Strausberg Germany, 1999.

[26] Z. Tu, Y. Lu, Evaluation of typical concrete material models used in hydrocodes for high dynamic response simulations, International Journal of Impact Engineering 36 (1) (2009) 132–146.

[27] W. Shin, H. Park, J. Han, Improvement of the dynamic failure behavior of concrete subjected to projectile impact using user-defined material model, Construction and Building Materials 332 (2022) 127343.

[28] S. Hanchak, M. Forrestal, E. Young, J. Ehrgott, Perforation of concrete slabs with 48 mpa (7 ksi) and 140 mpa (20 ksi) unconfined compressive strengths, International Journal of Impact Engineering 12 (1) (1992) 1–7.

[29] M. E. Abdel-Kader, Modified settings of concrete parameters in RHT model for predicting the response of concrete panels to impact, International Journal of Impact Engineering 132 (2019) 103312.